Sequencing of *FTO* and *ALKBH5* in men undergoing infertility work-up identifies an infertility-associated variant and two missense mutations

Miriam Landfors, M.Sc.,[a] Sigve Nakken, Ph.D.,[b] Markus Fusser, Ph.D.,[a] John-Arne Dahl, Ph.D.,[a] Arne Klungland, Ph.D.,[a] and Peter Fedorcsak, Ph.D.[c]

[a] Department of Microbiology, Institute of Medical Microbiology, Rikshospitalet; [b] Department of Tumor Biology, Institute for Cancer Research, Oslo University Hospital; and [c] Department of Gynecology, Oslo University Hospital and Institute of Clinical Medicine, University of Oslo, Oslo, Norway

Objective: To assess whether men with reduced semen quality exhibit genetic variants in the genes coding for the messenger RNA methylation erasers FTO and ALKBH5.
Design: DNA of men undergoing infertility work-up was extracted and the *FTO* and *ALKBH5* genes were sequenced. Statistical analysis was used to study the correlation between the identified *ALKBH5* and *FTO* variants and sperm quality.
Setting: University hospital infertility clinic.
Patient(s): Semen samples from 77 unselected men that had been referred to Oslo University Hospital for routine semen analysis as part of infertility work-up.
Intervention(s): Not applicable.
Main Outcome Measure(s): Immunohistochemistry and Western blot were used to confirm the presence of ALKBH5 and FTO in human testis. DNA extraction from samples was followed by Illumina MiSeq amplicon high throughput sequencing and sequence alignment. Variant calling was carried out using GATK's UnifiedGenotyper. Standard semen parameter analysis was performed according to World Health Organization guidelines.
Result(s): We found an *FTO* genetic variant to be associated with reduced semen quality. We also identified two *FTO* missense variants, one mutation (p.Cys326Ser) was located in the important linker between the two protein domains; the other mutation (p.Ser256Asn) was situated in a flexible loop able to interact with other molecules.
Conclusion(s): The discovery of two missense mutations with potentially detrimental effect on the functionality of the methylation eraser protein FTO, as well as a genetic variant of the same protein that is associated with altered semen quality could suggest that aberrant demethylation of messenger RNA is a factor involved in reduced male fertility. (Fertil Steril® 2016;105:1170–9. ©2016 The Authors. Published by Elsevier Inc. on behalf of the American Society for Reproductive Medicine. This is an open access article under the CC BY-NC-ND license (http://creativecommons.org/licenses/by-nc-nd/4.0/).)
Key Words: *ALKBH5*, *FTO*, mRNA methylation, 6-methyladenine, semen quality, infertility

Discuss: You can discuss this article with its authors and with other ASRM members at http://fertstertforum.com/landforsm-sequencing-fto-alkbh5-variants/

Use your smartphone to scan this QR code and connect to the discussion forum for this article now.*

* Download a free QR code scanner by searching for "QR scanner" in your smartphone's app store or app marketplace.

Received July 16, 2015; revised December 10, 2015; accepted January 6, 2016; published online January 25, 2016.
M.L. has nothing to disclose. S.N. has nothing to disclose. M.F. has nothing to disclose. J.-A.D. has nothing to disclose. A.K. has nothing to disclose. P.F. has nothing to disclose.
Supported by the Norwegian Research Council and Health South East Region Norway. Funding for open access charge: Norwegian Research Council; specifically, the Research Programme of the EEA/Norway Grants (grant POL/NOR/196258/2013).
Reprint requests: Peter Fedorcsak, Ph.D., Department of Gynecology, Oslo University Hospital and Institute of Clinical Medicine, University of Oslo, 0027 Oslo, Norway (E-mail: peter.fedorcsak@medisin.uio.no).

Fertility and Sterility® Vol. 105, No. 5, May 2016 0015-0282

http://dx.doi.org/10.1016/j.fertnstert.2016.01.002

During the past decades, declining sperm counts (1) and increasing incidence of testicular cancer (2) have increased concerns about deterioration of human fecundity (3). Although the causes of these secular trends remain to be ascertained, impaired sperm quality has been linked to genetic defects, in utero exposure to environmental pollutants, obesity, and advanced age (4).

Haploid spermatozoa are produced from undifferentiated primordial germ

cells through an elaborate process involving cell proliferation, meiosis, and transformation of spermatids to mature spermatozoa. During spermiogenesis, remodeling of chromatin and consequent termination of transcription necessitates a unique translational regulation, including synthesis, storage, and delayed translation of messenger RNA (mRNA) transcripts (5).

More than 100 structurally distinct RNA modifications have been identified in eukaryotes (6). The most prevalent of the internal mRNA modifications is N^6-methyladenosine (m^6A), which is distributed nonrandomly in approximately 25% of all transcripts (6, 7). Fluctuations in m^6A levels have been shown to influence stability, splicing, transport, and decay of mRNA, affecting meiosis, apoptosis, the length of the circadian clock, and maintenance of pluripotency (8–13).

We have recently shown that ALKBH5 demethylates mRNA m^6A in vivo (10). Notably, although *Alkbh5*$^{-/-}$ mice are indistinguishable from their wild-type littermates, we observed that male *Alkbh5*$^{-/-}$ mice have compromised fertility. The breeding success rate is remarkably low, the testes are smaller than wild-type, exhibiting extensive apoptosis and abnormal tubular anatomy (10). The spermatozoa are greatly reduced in number and display severely aberrant morphology and reduced motility (10). An additional AlkB homologue family member, the fat mass and obesity associated protein (FTO), has been reported to demethylate mRNA m^6A in mammalian cells (14, 15) and FTO-depleted cells exhibit higher levels of m^6A than control cells (11).

We report that the previously observed nuclear speckle localization of mouse ALKBH5 is conserved for human ALKBH5 in primary spermatocytes. Intrigued by the subfertility in *Alkbh5*$^{-/-}$ mice, the shared role of ALKBH5 and FTO as m^6A erasers in mRNA, and the intricate RNA processing during spermiogenesis, we examined whether sequence variants of the *ALKBH5* and *FTO* genes were related to semen quality. We sequenced the exons, splice sites, and 5′ and 3′ untranslated regions (UTRs) of *FTO* and *ALKBH5* in men undergoing infertility work-up, using the Illumina TruSeq Custom Amplicon assay and the MiSeq platform (Illumina, Inc.). Single nucleotide variants and short indels were determined using GATK's UnifiedGenotyper and factor analysis was used to correlate sperm quality parameters with the variants. We identified one variant in *FTO* that is inversely correlated to semen quality and describe two *FTO* missense variants.

MATERIALS AND METHODS

Testis Protein Extract

Human testicular tissue samples were obtained by percutaneous needle biopsy after written informed consent (see section on Patient selection and ethical approval). The patients underwent routine diagnostic procedure for obstructive azoospermia. The samples were stored at −80°C before the experiment. Thawed samples were cut into smaller pieces with scissors, 0.75 mL of RIPA buffer (0.5% sodium dodecyl sulfate [SDS], 1% NP40, 1 × Complete Protease Inhibitor [Roche], 0.1 mM phenylmethylsulfonyl fluoride [PMSF] in phosphate-buffered saline [PBS]) was added to 100 mg of tissue, and homogenized with a FastPrep-24 instrument (MP Biomedicals), speed 4 for 30 seconds. The mixture was incubated on ice for 30 minutes and then centrifuged for 30 minutes at 16,900 relative centrifugal force. The supernatant containing the whole cell extract was frozen at −80°C.

Western Blot

Human testis biopsy whole cell extracts were mixed with 10% 1,4-dithiothreitol (Cleland's reagent) (DTT) (1 M), 1 × lithium dodecyl sulfate, and distilled H_2O, heat-denatured at 90°C for 10 minutes and then cooled on ice. The mixtures containing 10 and 20 μg of protein of whole cell extract were loaded on a 12% NuPAGE Gel (Life Technologies), electrophorized at 200 V for approximately 45 minutes, and transferred to a nitrocellulose membrane using a Transblot-Turbo blotter (BioRad) for 15 minutes. The membrane was blocked at room temperature for approximately 1 hour in PBST-M (5% milk in phosphate-buffered saline with 0.05% Tween 20) on a shaker. Primary anti-FTO antibody (1:3,000 in PBST-M), as previously reported (14) was added and incubated for 1 hour at room temperature on a shaker. Three times of 10-minute PBST washes followed. Secondary horseradish peroxidase-conjugated goat anti-rabbit antibody (catalogue no. Ab6721, AbCam) was diluted 1:40,000 in PBST-M and incubated at room temperature for 1 hour on a shaker. Three times of 10-minute PBST washes followed. The membrane was washed for 5 minutes in PBS. SuperSignal West Extended Duration Substrate (ThermoScientific) was added to the membrane. The bands were visualized with Gel Doc apparatus (Bio-Rad).

Immunofluorescence

Testicular biopsy tissue samples were immediately set in optimum cutting temperature compound (Sakura), frozen in liquid nitrogen, and sectioned at 5 μm with a cryotome. Sections were fixed in cold acetone and exposed to primary antibodies (anti-ALKBH5 [10], 1:200; normal rabbit IgG, Santa Cruz, 1:200; anti-SC35, Abcam, 1:50; anti-FTO, Epitomics, 1:1,000; anti-vimentin, Abcam, 1:100) in 1% bovine serum albumin (BSA)/PBS, followed by fluorochrome-labeled secondary antibodies (1:1,000) in 10% BSA/PBS.

Patient Selection and Ethical Approval

The protocol of the study was approved by the Regional Committee for Research Ethics (No. 2011/913). We invited 100 consecutive patients to participate and obtained written informed consent. Patients had been referred to Oslo University Hospital Rikshospitalet for routine semen analysis as part of infertility work-up. Patients with azoospermia were excluded for the following reasons: lack of quantitative sperm parameters for calculating factor analysis; uncertainty whether the patient had obstructive azoospermia with normal spermatogenesis or nonobstructive azoospermia with impaired spermatogenesis, as anamnestic information is not routinely available to the laboratory at this stage; reduced DNA quantity and quality in seminal fluid in azoospermia; if azoospermia cases were retained in the analysis, some variables would have bimodal distributions; last, we chose to sequence sperm DNA, thereby excluding patients with azoospermia from the samples that underwent analysis of

ALKBH5/*FTO* variants. Samples were collected during the period of January 9, 2011 to March 10, 2011. An aliquot of semen was frozen at −80°C for DNA extraction. Of the initial 100 patients, 93 met the aforementioned criteria regarding azoospermia. Due to failures during the sequencing process, only 77 patients with complete datasets contributed to the final analysis.

Semen Analysis

Semen analysis was performed according to the World Health Organization guidelines (16) with some modifications. Briefly, the ejaculate was collected in sterile sample containers by masturbation, allowed to liquefy under continuous shaking at 37°C for 30 minutes when volume, pH, and viscosity were measured. Motility of >200 spermatozoa was scored according to the World Health Organization guidelines on a phase-contrast microscope fitted with a heated stage and counting reticle. Sperm concentration was determined in Neubauer chambers (Improved Neubauer counting chamber, Karl Hecht) using appropriately diluted samples. The presence of anti-sperm IgG and IgA antibodies was assessed with the SpermMAR test (FertiPro). For assessment of sperm morphology, semen samples were smeared on glass slides, fixed in ethanol, and stained according to the modified Papanicolaou procedure. More than 200 spermatozoa were counted per slide and the presence of defects at the head, neck, tail, as well as cytoplasmic droplets were recorded according to the strict criteria (17). The andrology laboratory participated in the European Society of Human Reproduction and Embryology Special Interest Group in Andrology, (ESHRE)-SIGA, external quality control scheme. Sperm DNA fragmentation and DNA stainability were assessed by flow cytometry in permeabilized acid-treated spermatozoa using acridine orange staining according to the procedure of Evenson and Jost (18).

Factor Analysis of Semen Parameters

During diagnostic work-up, infertile men routinely undergo standard semen analysis, which implies assessment of multiple parameters related to sperm density and function, such as concentration, motility, and morphology. We extracted anonymized records of 6,049 men who had undergone semen analysis in our laboratory according to established guidelines (16). All men in the population of 6,049 had been referred to sperm analysis as part of infertility work-up. We excluded other referral reasons, including postvasectomy tests, sperm cryopreservation before gonadotoxic treatment, repeated sperm analysis after previously recognized abnormality. We argued that an unselected sample of patients referred for infertility work-up will comprise men with varying levels of sperm quality. When compared to World Health Organization reference values, 2,740 (45%) patients had normal semen parameters, whereas 1,936 (32%) had one, 1,002 (16%) two, and 371 (6%) men had three semen features (concentration, motility, or morphology) outside the reference range. This prevalence of sperm defects is comparable to the reported frequency of sperm analysis abnormalities (31% for one, 18% for two, and 10% for three abnormal sperm parameters) in subfertile couples (19).

Sperm parameters obtained from the population sample (n = 6,049) were further processed with factor analysis to simplify the dataset and derive a single variable that can be used to assess the association between genotype and sperm quality. First, we examined correlation among 14 selected continuous semen parameters and affirmed, as expected, that the various parameters were closely inter-related (Supplemental Fig. 1A). Second, we applied factor analysis to the semen parameters and constructed four independent, noncorrelating factors from the data (Supplemental Fig. 1B). These four factors collectively accounted for 54.5% of the total variance. Maximum-likelihood factor analysis was performed using the factanal function of R (version 3.1.2; R Foundation for Statistical Computing). The factor scores were scaled so that these have normal distribution of mean = 0 and SD = 1 (variance = 1). Negative scores indicated association with inferior sperm quality (Supplemental Fig. 1B). We also calculated the mean of factors and argued that mean of factors can be used to classify patients according to semen quality rather than relying on measured semen parameters. Third, we performed sensitivity analysis to affirm the contribution of individual sperm parameters to factors. We omitted sperm parameters one-by-one from the dataset, re-run factor analysis and calculated mean factor scores, which were compared to the full model using the r^2 statistics (Supplemental Fig. 1C). The association of mean factor scores and sequence variants was examined with linear regression analysis.

DNA Extraction

Human semen samples were pelleted by centrifugation for 20 minutes at 8,000 × *g* and 4°C. The pellets were resuspended in lysis buffer (10 mM Tris-HCl, at pH 8.0, 5 mM ethylenediaminetetraacetic acid [EDTA], 1% SDS), DTT was added to a final concentration of 100 mM and the samples were incubated at 37°C for 30 minutes. RNase A (100 μg) was added and the samples were again incubated at 37°C for 30 minutes. Proteinase K was added to a final concentration of 1 mg/mL. The samples were then incubated at 55°C overnight on a shaker. Genomic DNA was extracted with Qiagen Blood and Tissue kit (Qiagen) according to manufacturer's instructions. The DNA was stored at −80°C and delivered for sequencing at a concentration of 50 ng/μL and a volume of 12 μL.

Sequencing and Variant Calling

We used the Illumina MiSeq amplicon technology at the sequencing facility at Radiumhospitalet in Oslo, Norway, to identify germ-line variants in *ALKBH5* and *FTO* (see schematic overview in Supplemental Fig. 2). Primers were designed to generate amplicons covering the exonic regions as well as parts of the UTRs (Supplemental Fig. 3); the primer sequences and the targeted genomic regions can be found in Supplemental Tables 1 and 2. Sequence alignments were made using the Illumina TruSeq Custom Amplicon workflow, using a banded Smith-Waterman algorithm. Single nucleotide variants and short indels were determined using GATK's UnifiedGenotyper (version 3.2.3), using the following nondefault options: *−max_alternate_alleles=2, −standard_min_confidence_threshold_for_emitting=10* (minimum phred-scaled

confidence threshold at which variants should be emitted), *–genotype_likelihoods_model=BOTH* (single nucleotide polymorphisms and indels). To reduce the number of false positives among the identified variants, we set up a hard filter of genotypes according to GATK's best practices (genotypes that were kept needed the following GATK genotype scores: QualByDepth >2.0, FisherStrand <60.0, RMSMappingQuality >40, MQRankSum > −12.5, ReadPosRankSum > −8). Heterozygotes in which the read fraction of the alternative allele was <20% were also discarded as false positives.

To interpret the functional role of identified variants, we implemented a functional annotation pipeline of genomic variants. This included ANNOVAR—August 2014 release (20) for consequence type with respect to gene-coding regions (using RefSeq as the model database for human genes/proteins), PFAM version 27.0 (21) for overlap with functional protein domains, UniProt Knowledge base (22) for overlap with active and functional sites within proteins, dbNSFP version 2.6 (23) for computational predictions of phenotypic effects of missense variants, and dbSNP version 142 (24) for overlap with previously reported germ-line variants. We also checked for overlap with 1000Genomes Project phase3 (1000 Genomes Project Consortium 2010) and the ExAC database (Exome Aggregation Consortium 2015) for population-specific allele frequencies of germ-line variants.

RESULTS

FTO and ALKBH5 are Present in the Human Testis

RNA adenine is methylated by methyltransferases, and the resulting m^6A base can be converted back to adenine by demethylases. Two mRNA m^6A demethylases are known to date, FTO and ALKBH5. These use dioxygen, ferrous iron, and α-ketoglutarate as cofactors (Fig. 1A). We wanted to confirm

FIGURE 1

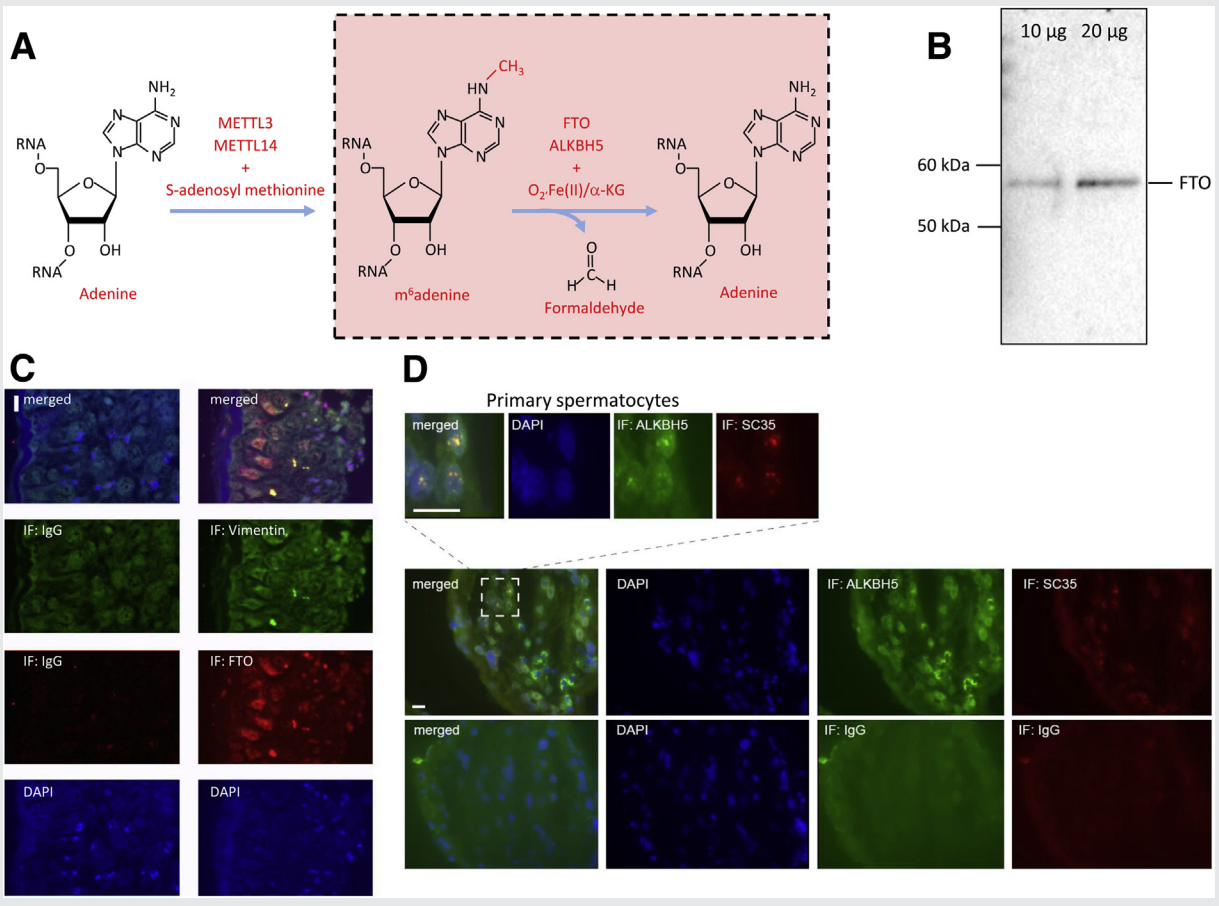

FTO and ALKBH5 are N^6-methyladenosine RNA demethylases present in human testis. (**A**) Adenine is converted to m^6adenine through the catalytic activity of methyltransferases METTL3 and METTL14 using S-adenosyl methionine. m^6adenine is converted back to adenine by the demethylases FTO and ALKBH5 using dioxygen, ferrous iron, and α-ketoglutarate (O_2-Fe(II)/α-KG) as cofactors. (**B**) Immunoblotting of human testis whole cell extract (WCE) with FTO antibody, *numbers* indicate molecular weight in kilodaltons. Lane 1, 10 μg WCE; lane 2, 20 μg WCE. (**C**) Immunofluorescence image of human testis section stained with 6-diamino-2-phenylindole (DAPI) and antibodies targeting FTO and vimentin. Scale bar, 10 μM. (**D**) Immunofluorescence image of human testis biopsy section stained with DAPI and antibodies targeting ALKBH5 and the nuclear speckle protein SC35. *Lower images*: IgG as negative control. Scale bar, 10 μM.

Landfors. Sequencing of FTO *and* ALKBH5 *variants. Fertil Steril 2016.*

that these demethylating enzymes are present in the human testis. To this end, whole cell extract from human testis was immunoblotted against FTO, and a specific band was obtained at 58 kDa corresponding to the expected molecular weight of the FTO protein (Fig. 1B). In addition, immunofluorescence staining of human testis sections for FTO detected FTO in the testis, with a stronger signal in the Sertoli cells (Fig. 1C). The presence of ALKBH5 in human testis was confirmed using immunofluorescence staining of sectioned biopsy samples. ALKBH5 is primarily localized to the nucleus and colocalizes with the nuclear speckle marker SC35 in primary spermatocytes (Fig. 1D). The presence of primary spermatocytes was affirmed in adjacent sections by typical pattern of 6-diamino-2-phenylindole (DAPI)-stained nuclear material and cells' position within the seminiferous tubules. Normal rabbit IgG was used as a negative control.

Identification of Sequence Variants in the *ALKBH5* and *FTO* Genes

To identify sequence variants of *ALKBH5* and *FTO*, we recruited 77 unselected men who were referred to semen analysis as part of infertility work-up. Patients gave written informed consent and delivered a semen sample that was analyzed according to routine procedures. Semen quality factors were calculated as described in the Materials and Methods section. Based on the distribution of the mean of factors, this sample of 77 men was representative of the total population of 6,049 men undergoing infertility work-up at our clinic (Supplemental Fig. 4). The men were invited to the study consecutively, ensuring an unbiased random recruitment, and the distribution of the mean factor scores in the sample of 77 men fitted well with the factor score distribution of the whole population of 6,049 men (Kolmogorov-Smirnoff test, $P=.79$), indicating that sperm quality was comparable. Genomic DNA extracted from the semen samples was purified and sequenced. The sequencing scheme involved multiplex polymerase chain reaction (PCR), high-throughput sequencing, mapping and variant identification, as outlined in Supplemental Figure 2. Sequencing of selected regions of the *ALKBH5* and *FTO* genes identified 33 sequence variants, 21 were found in the *ALKBH5* gene and 12 in the *FTO* gene (Table 1). One variant upstream of the *FTO* transcription start site overlapped an intron of *RPGRIP1L*. Of all the identified variants, 29 were previously reported in the dbSNP database (24). The four variants that were not previously reported in dbSNP consisted of three short deletions (all located in the UTR of *FTO*), and one single nucleotide variant (*FTO* coding region). With respect to protein-coding changes, we identified two missense variants in the *FTO* gene (p.Ser256Asn and p.Cys326Ser), each occurring once in the sample cohort. Missense variants generate a modified amino acid sequence in the expressed FTO protein. Although p.Cys326Ser was not reported in dbSNP, we discovered that it was recorded as a very rare allele in the Exome Aggregation (ExAC) database, with an estimated global population frequency of 0.0001 (25). The other missense variant (p.Ser256Asn) was also present in the ExAC database, with an estimated global population frequency of 0.002. Both protein-coding variants were thus generally rare in the global population. Of the variants found in the *ALKBH5* gene, the majority were located in the 3′ UTR (Table 1).

Association Between Variants and Semen Quality

The group of 77 men was arranged by increasing semen quality based on the mean of factors (Fig. 2). Association among sequence variants of *ALKBH5* and *FTO* and the mean of factors was assessed by linear regression analysis. The *FTO* single nucleotide variant rs62033438, carried by 48 samples, is an intronic variant that was found to be significantly associated with semen quality ($P=.001$), suggesting that the presence of the wild-type (A) compared with the variant (G) nucleotide was related to inferior semen quality (Table 1). Of the sequenced patients, 29 exhibited genotype A/A, 38 exhibited genotype G/A, and 10 exhibited genotype G/G. Sperm concentration, total sperm count, normal DNA stainability, normal sperm morphology, and rapid progressive motility were positively associated with the presence of G/G or G/A genotype in rs62033438 (Supplemental Fig. 5).

Protein Structure Analysis of Missense Mutations in *FTO*

As mentioned previously, two rare missense mutations were identified in the *FTO* gene: p.Ser256Asn and p.Cys326Ser (Fig. 3). The three-dimensional structure of human FTO can be found in the Protein Data Bank under the accession code 3LFM (26). This crystallized structure is an amino terminally truncated (by 31 residues) version of the human FTO protein bound to the mononucleotide 3-meT (26). The three-dimensional structure of human FTO contains Fe^{2+}, a bound nucleotide and an α-ketoglutarate analogue. Residues 251–263 form a loop that is not visible in the X-ray structure because it is structurally disordered and flexible, and does not fold into a regular three-dimensional structure. The loop is, however, highly accessible and able to interact with other macromolecules and molecular surfaces. The missense mutation p.Ser256Asn, which we observed in the germ line of a patient, is located in the middle of this loop. The structure comprises an amino-terminal α-ketoglutarate-dependent dioxygenase domain and a carboxy-terminal domain that appears to be unique to FTO. The p.Cys326Ser variant is located in the very middle of the linker between these two domains.

DISCUSSION

Although the male factor is a contributing cause in about 50% of infertile couples, the determinants of impaired semen quality, especially the genetic causes, often remain undiagnosed (27). In addition to chromosome abnormalities and single gene defects in rare and severe cases of male sterility (28), more common gene polymorphisms also affect fertility (29). In the present study, by combining deep sequencing and robust statistical analysis, we explored whether sequence variants of *ALKBH5* and *FTO* genes, which are involved in RNA processing and spermatogenesis in mice, were associated with semen quality in humans.

TABLE 1

Sequence variants of *ALKBH5* and *FTO*, variant frequency, and association with semen quality.

Variant symbol	Locus	Genomic position (GRCh37)	Variant class	Alleles	Amino acid change	Variant type	Genotype frequency[a] 0/0	0/1	1/1	Association with semen quality (*P* value)
rs78123366	*ALKBH5*	Chr17:18086495	Snv	G/A		Upstream gene variant	76	1	0	1.95E-01
rs552236280	*ALKBH5*	Chr17:18086570	Snv	C/T		Upstream gene variant	75	2	0	8.74E-01
rs558358916	*ALKBH5*	Chr17:18086716	Snv	A/G		Upstream gene variant	76	1	0	4.47E-01
rs146551631	*ALKBH5*	Chr17:18086951	Snv	G/A		5′ UTR variant	76	1	0	1.27E-01
rs1064629	*ALKBH5*	Chr17:18087299	Snv	C/T		5′ UTR variant	58	17	2	6.73E-01
*087513[b]	*ALKBH5*	Chr17:18087513	Indel	TGCCCCGCCC/T		5′ UTR variant	76	1	0	3.39E-02
rs11078411	*ALKBH5*	Chr17:18088094	Snv	C/T	p.H179H	Synonymous variant	72	2	3	4.73E-01
rs1563371	*ALKBH5*	Chr17:18111793	Snv	C/T		3′ UTR variant	45	29	3	7.31E-01
rs142135062	*ALKBH5*	Chr17:18111802	Indel	GTTTTTGT/G		3′ UTR variant	35	29	13	7.95E-01
rs1378602	*ALKBH5*	Chr17:18111868	Snv	G/A		3′ UTR variant	14	36	27	7.65E-01
rs181356656	*ALKBH5*	Chr17:18111980	Snv	G/A		3′ UTR variant	76	1	0	4.37E-01
rs570534770	*ALKBH5*	Chr17:18111998	Snv	A/C		3′ UTR variant	76	1	0	6.20E-01
rs13284	*ALKBH5*	Chr17:18112130	Snv	C/T		3′ UTR variant	45	29	3	7.31E-01
*112369[b]	*ALKBH5*	Chr17:18112369	indel	GC/G		3′ UTR variant	76	1	0	3.00E-01
rs113683457	*ALKBH5*	Chr17:18112432	Snv	A/G		3′ UTR variant	70	7	0	7.85E-01
rs3088233	*ALKBH5*	Chr17:18112675	Snv	C/T		3′ UTR variant	45	29	3	7.31E-01
rs4925146	*ALKBH5*	Chr17:18112720	Snv	G/T		3′ UTR variant	76	1	0	1.27E-01
rs199923993	*ALKBH5*	Chr17:18112836	indel	AATAAT/A		3′ UTR variant	76	1	0	7.95E-01
rs8400	*ALKBH5*	Chr17:18112845	Snv	G/A		3′ UTR variant	3	18	56	6.08E-01
rs116946161	*ALKBH5*	Chr17:18113027	Snv	G/A		3′ UTR variant	76	1	0	7.95E-01
*113162[b]	*ALKBH5*	Chr17:18113162	indel	A/AT		3′ UTR variant	1	76	0	3.39E-02
rs62048369	*FTO*	Chr16:53737560	Snv	G/A		Intron variant	74	3	0	4.05E-01
rs3826169	*FTO*	Chr16:53860481	Snv	G/A		Intron variant	7	27	43	9.60E-01
rs144743617	*FTO*	Chr16:53878082	Snv	G/A	p.S256N	Missense variant	76	1	0	8.71E-02
rs62033438	*FTO*	Chr16:53878247	Snv	A/G		Intron variant	29	38	10	1.04E-03
rs143719235	*FTO*	Chr16:53913678	Snv	T/C		Intron variant	75	2	0	6.52E-01
*913756[b]	*FTO*	Chr16:53913756	Snv	T/A	p.C326S	Missense variant	76	1	0	5.14E-01
rs552126057	*FTO*	Chr16:54145602	Snv	C/T		Intron variant	76	1	0	8.24E-01
rs5816925	*FTO*	Chr16:54147206	indel	CG/C		3′ UTR variant	13	35	29	6.00E-02
rs147409759	*FTO*	Chr16:54148007	Snv	G/T		3′ UTR variant	75	2	0	7.34E-01
rs117637522	*FTO*	Chr16:54148037	Snv	A/A		3′ UTR variant	76	1	0	1.95E-01
rs79234192	*FTO*	Chr16:54148128	Snv	G/A		3′ UTR variant	76	1	0	9.92E-01
rs45564131	*FTO*	Chr16:54148189	Snv	A/AT		3′ UTR variant	75	2	0	7.34E-01

Note: indel = insertion/deletion variant; Snv = single nucleotide variant.
[a] 0/0 = wild-type reference allele (monomorphic); 0/1 = heterozygous alternative allele; 1/1 = homozygous alternative allele.
[b] Variants not previously reported in the dbSNP database.

Landfors. Sequencing of FTO *and* ALKBH5 *variants. Fertil Steril 2016.*

FIGURE 2

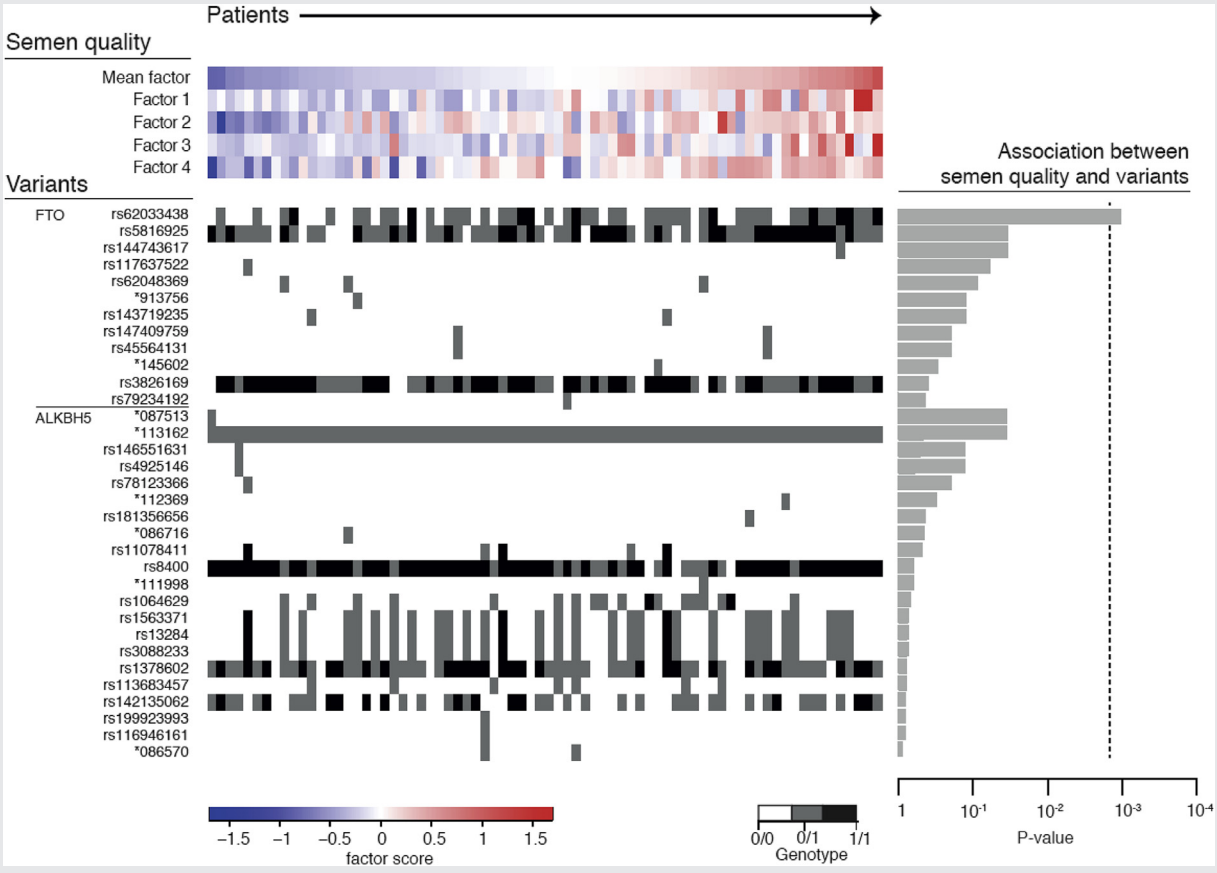

Correlation between sequence variants of ALKBH5 and FTO and semen quality. Men, who are not azoospermic, undergoing infertility work-up (n = 77) are grouped by increasing semen quality as defined by the mean of four independent factors established by factor analysis on the larger population (*top*: *red-blue scale* indicates factor scores). Illumina MiSeq sequencing of selected regions of *ALKBH5* and *FTO* identifies 33 sequence variants. *Bottom right*: *white*, *gray*, and *black* indicate wild-type, heterozygote, and homozygote variant genotypes, respectively. Presence of variant rs62033438 is significantly associated with semen quality (linear regression, uncorrected *P*=.001; *dashed line* indicates level of Bonferroni-corrected $\alpha<0.05$).

Landfors. Sequencing of FTO *and* ALKBH5 *variants. Fertil Steril 2016.*

The transformation of the spermatids during spermiogenesis comprises a condensation of nuclear DNA. This complicated process involves a wave of transcription that generates mRNAs needed during later stages when transcription has been largely shut down due to inaccessible DNA. This distinct mRNA processing is vital for the accurate progression of the spermiogenesis (30).

Proper regulation of the mRNA methylation level is essential for cellular function, demonstrated by the fact that depletion of methylating or demethylating enzymes both result in apoptosis (10, 31). Nonstoichiometric distribution along the mRNA transcripts, absence in poly(A) tails, a consensus sequence that is conserved across kingdoms, and differences in abundance between tissues, strongly suggest a regulated, functional role for m^6A (15, 32). At present, two m^6A demethylating enzymes have been identified, ALKBH5 and FTO. They belong to the human AlkB homologue family of nonheme iron- and α-ketoglutarate-dependent dioxygenases (33, 34). Depletion of these enzymes results in higher m^6A levels (10, 11).

The importance of proper methylation of mRNA for meiosis and development has been shown in a number of reports. m^6A methylation plays a critical role in yeast meiosis with impaired meiotic progression occurring as a result of compromised methylation activity (8). Disruption of the m^6A methylating agent in *Arabidopsis thaliana* leads to embryo lethality (32) and methylating components in *Drosophila melanogaster* have been shown to be essential for oogenesis (35).

Consistent with the finding that aberrant m^6A processing compromises meiosis, mice deficient in ALKBH5 displayed spermatogenic maturation arrest (10). Expression of *Alkbh5* has been detected in all mouse organs tested; the highest expression was found in testis (10). The mRNA nuclear export is greatly affected in ALKBH5-deficent cells with a significant shift in mRNA localization from the nucleus to the cytoplasm. It appears to be the demethylating ability of ALKBH5 that causes this shift (10). Extensive cell death through apoptosis was discovered in the testes of $Alkbh5^{-/-}$ mice (10). In the testes of wild-type mice, ALKBH5 colocalizes with splicing

FIGURE 3

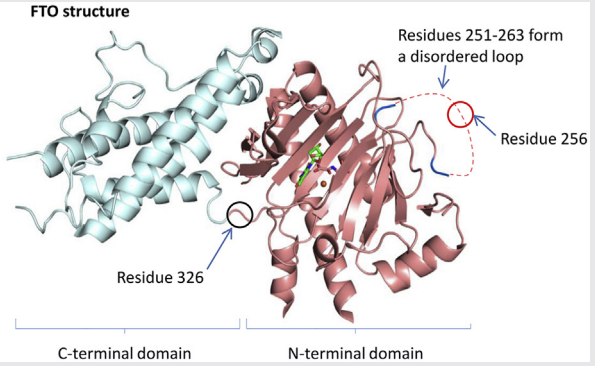

Structure of FTO with positions of observed missense mutations, variants rs144743617 and *913756 indicated. The crystallized three-dimensional structure of human FTO comprises an amino terminal α-ketoglutarate-dependent dioxygenase domain (*salmon*) and a carboxyl terminal domain that appears to be unique to FTO (*cyan*). The structure also contains Fe^{2+} (*orange ball*), a bound nucleotide (*green*), and an α-ketoglutarate analogue (*salmon*, *red*, and *blue sticks*). Variant rs144743617: mutation p.Ser256Asn. Residues 251–263 form a flexible loop that is not visible in the X-ray structure (*dashed line*). Residues 249 and 250 as well as residues 264 and 265 flank the loop and are depicted in *blue*. Residue Ser256 is located in the middle of this loop (*red circle*). Variant *913756: mutation p.Cys326Ser. Residue 326 (*black circle*) is located exactly in the middle of the linker between the two FTO domains. Protein Data Bank, accession code 3LFM (Han et al. 2010). The protein illustrations were generated with PyMOL (http://www.pymol.org).

Landfors. Sequencing of FTO *and* ALKBH5 *variants. Fertil Steril 2016.*

proteins in nuclear speckles where storage and pre-mRNA processing occurs and is specifically expressed in primary spermatocytes (10, 36). We show here that human testes display the same pattern of expression: ALKBH5 is expressed in the testes and appears to be specifically present in primary spermatocytes where it colocalizes with the nuclear speckle marker SC35. This conservation is underpinning the plausibility of a conserved functional role of ALKBH5 in human spermatogenesis.

Both in murine and human tissue samples *FTO* was found to be widely expressed in fetal and adult tissues, with highest expression in the brain, particularly the hypothalamus (37, 38). FTO has repeatedly been shown to be localized to the nucleus (38, 39); however, a cytoplasmic fraction might also exist (40). Similarly to the *Alkbh5*$^{-/-}$ mice, *Fto* knockout mice exhibit severely reduced fertility (Ulrich Rüther, Heinrich-Heine-University, Düsseldorf, Germany, unpublished data). We confirmed the expression of FTO in human testis; this is consistent with previous findings (The Human Protein Atlas, www.proteinatlas.org [41]). Considering that the localization of m^6A in the mRNA fragments is highly conserved between mice and humans (31), and that a shift in the m^6A levels in *Alkbh5*$^{-/-}$ mice seems to adversely affect spermatogenesis, a malfunctioning FTO protein may also affect fertility.

Although there is evidence for low levels of late transcriptional activity during spermiogenesis (42, 43), the bulk of the mRNA of spermiogenesis-specific proteins are transcribed early during spermatogenesis and stored as translationally repressed mRNAs that are translated in elongating spermatids (30, 44). The repressed mRNAs are stored and processed in a germ cell-specific cellular structure called the chromatoid body (44). The chromatoid body has been described to share a number of significant similarities with the processing body (P-body) and function as a sorting center for mRNAs in male germ cells (44, 45). It has been shown that m^6A is recognized by the human YTH domain family 2 protein (YTHDF2) and that this methylation-dependent interaction leads to the bound mRNA, localizing to sites of mRNA decay such as the P-body (46). This poses the question whether mRNA is transported to the chromatoid body in a similar way and that this process could be disturbed by the lack or reduced presence of demethylating proteins. The proteins necessary for the later steps in spermiogenesis, including flagellum formation, must be synthesized and stored before the event takes place. Defects in the storage or processing of the corresponding mRNAs could therefore impact the efficiency and accuracy of the morphological change, including tail development. The spermatozoa of ALKBH5 deficient mice exhibit morphological defects including tail abnormalities. Notably, sperm morphological defects are exceptionally prevalent in infertile men (47).

Of the 21 variants identified in the *ALKBH5* gene, 14 were localized to the 3′ UTR. The 3′ UTR is one of the major gene-regulating regions (48). The 3′ UTRs contain binding sites for micro RNAs, as well as a large number of regulatory proteins (48). There are indications that the length of the 3′ UTR is an important factor in mRNA expression with longer regions having a higher probability of containing regulatory sites that impact translation (48). The 3′ UTR of human *ALKBH5* is1,555 nucleotides long (http://www.ncbi.nlm.nih.gov/IEB/Research/Acembly/av.cgi?exdb=AceView&tdb=36a&term=ALKBH5). This exceeds the average mammalian 3′ UTR of approximately 1,000 nucleotides (49–51). The numerous variants found in the 3′ UTR of our patients could reflect a change in the processing of the *ALKBH5* mRNA due to misfolded secondary structures, or disruption of sites for micro RNAs or RNA-binding proteins.

Both FTO and ALKBH5 have been reported to contain the double-stranded β-helix fold typical for their protein family, as well as structures that convey selectivity toward single-stranded nucleotide substrates (26, 38, 52). Human FTO consists of an amino-terminal α-ketoglutarate-dependent dioxygenase domain (residues 1–326) and a carboxy-terminal domain (residues 327–505). The latter appears to be unique to FTO, not sharing significant homology with any known structures (26).

In the present study we discovered two missense variants in the *FTO* gene in germ line DNA from two patients. At amino acid position 256 a serine residue has been replaced by an asparagine (p.Ser256Asn). Residues 251–263 form a loop that is not visible in the X-ray structure because it is structurally disordered and flexible, and does not fold into a regular three-dimensional structure. The missense mutation p.Ser256Asn is located in the middle of this loop. Ser256 is conserved in placental mammals, implying a conserved

function. The variant has been described before and shown not to be correlated to obesity (53). In placental mammals, the region corresponding to human FTO residues 250–260 is highly enriched in negatively charged residues, Glu and Asp, as well as Gly and Pro. It is highly accessible and able to interact with other macromolecules, positively charged surfaces or similar. The change from one polar amino acid residue to another might not affect the charge of the residue; however, the accessibility of the residue to other macromolecules enables protein modifications, such as phosphorylation and glycosylation, that could be influenced by a residue change. The patient carrying the variant S256N had normozoospermia (concentration 107 M/mL, progressive motility 56%, normal forms >7%, high DNA stainability 5%). The patient had proven fertility.

The second missense variant identified in the present study is at amino acid position 326. A cysteine residue that has been replaced by a serine (p.Cys326Ser). p.Cys326 is located exactly in the middle of the linker between the two main FTO domains and is conserved in all mammals. The side-chain does not appear to interact with any other parts of the protein, at least not in the final, folded protein. Cys326 is not close to the active site or to the entrance to the active site pocket. There is extensive interaction between the two main domains of the FTO protein. This interaction is required for FTO catalytic activity (26). It has been suggested that the carboxyl domain stabilizes the conformation of the catalytically active amino domain (26). Interestingly, mutations that have been suggested to alter the interaction between the carboxy- and the amino-terminal domains. They have been shown to markedly reduce FTO activity (26). In an enzyme where the interaction between the two main domains is crucial for the activity of the protein, a change in the linker between these domains, as observed in our study, could have a profound effect on protein function. A homozygote loss-of-function mutation is not likely to be found, as loss-of-function mutations in humans have been reported to result in a severe phenotype of microcephaly, functional brain deficit, and psychomotor delay. The afflicted individuals do not survive the age of 30 months (54). The patient with variant C326S had isolated teratozoospermia (concentration 26 M/mL, progressive motility 41%, normal forms 1%, high DNA stainability 33%). We reviewed the patient's archived sperm smear and saw variable, grossly irregular head morphology, such as spermatozoa with irregular head shape, increased nuclear staining, irregular acrosome, exfoliated irregular germ cells, and occasionally double-headed or double-tailed spermatozoa indicating meiotic nondisjunction. Nonetheless, these morphological derangements are frequently seen in abnormal sperm smears and fail to define a distinct disease picture. The patient delivered two sperm tests with similar results, but the couple has not followed up the findings in our clinic. Further biochemical analysis should focus on assessing the degree of enzymatic functionality of these missense *FTO* variants.

The variant identified in the *FTO* gene that is associated with semen quality is an intronic variant. It is unlikely that an intronic variant changes the capability of the translated protein. However, intronic variants in the *FTO* gene have been shown to have an impact on the promoters of at least one other gene through long-range looping (55). Also, single nucleotide variants might not lead to functional mutations but could cause a shift in the transcription of the gene. Of the numerous gene polymorphisms implicated in male factor infertility, those affecting the *AZF* and the *MTHFR* have been independently confirmed to have clinical impact (56). Further studies are required to elucidate the functional mechanism causing an *FTO* variant to be associated with altered semen quality.

Acknowledgments: We thank Leonardo A. Meza-Zepeda and Susanne Lorenz for initial discussion and the services provided; Jon Lærdahl for help with protein structure analysis; Alexander Rowe for initial discussion; and Karin Margaretha Gilljam for proofreading.

REFERENCES

1. Carlsen E, Giwercman A, Keiding N, Skakkebaek NE. Evidence for decreasing quality of semen during past 50 years. BMJ 1992;305:609–13.
2. Shanmugalingam T, Soultati A, Chowdhury S, Rudman S, van Hemelrijck M. Global incidence and outcome of testicular cancer. Clin Epidemiol 2013;5:417–27.
3. Jensen TK, Sobotka T, Hansen MA, Pedersen AT, Lutz W, Skakkebaek NE. Declining trends in conception rates in recent birth cohorts of native Danish women: a possible role of deteriorating male reproductive health. Int J Androl 2008;31:81–92.
4. Joffe M. What has happened to human fertility? Hum Reprod 2010;25:295–307.
5. Kleene KC. Connecting cis-elements and trans-factors with mechanisms of developmental regulation of mRNA translation in meiotic and haploid mammalian spermatogenic cells. Reproduction 2013;146:R1–19.
6. Cantara WA, Crain PF, Rozenski J, McCloskey JA, Harris KA, Zhang X, et al. The RNA Modification Database, RNAMDB: 2011 update. Nucleic Acids Res 2011;39:D195–201.
7. Meyer KD, Jaffrey SR. The dynamic epitranscriptome: N6-methyladenosine and gene expression control. Nat Rev Mol Cell Biol 2014;15:313–26.
8. Schwartz S, Agarwala SD, Mumbach MR, Jovanovic M, Mertins P, Shishkin A, et al. High-resolution mapping reveals a conserved, widespread, dynamic mRNA methylation program in yeast meiosis. Cell 2013;155:1409–21.
9. Fustin JM, Doi M, Yamaguchi Y, Hida H, Nishimura S, Yoshida M, et al. RNA-methylation-dependent RNA processing controls the speed of the circadian clock. Cell 2013;155:793–806.
10. Zheng G, Dahl JA, Niu Y, Fedorcsak P, Huang CM, Li CJ, et al. ALKBH5 is a mammalian RNA demethylase that impacts RNA metabolism and mouse fertility. Mol Cell 2013;49:18–29.
11. Zhao X, Yang Y, Sun BF, Shi Y, Yang X, Xiao W, et al. FTO-dependent demethylation of N6-methyladenosine regulates mRNA splicing and is required for adipogenesis. Cell Res 2014;24:1403–19.
12. Wang Y, Li Y, Toth JI, Petroski MD, Zhang Z, Zhao JC. N6-methyladenosine modification destabilizes developmental regulators in embryonic stem cells. Nat Cell Biol 2014;16:191–8.
13. Geula S, Moshitch-Moshkovitz S, Dominissini D, Mansour AA, Kol N, Salmon-Divon M, et al. m6A mRNA methylation facilitates resolution of naive pluripotency toward differentiation. Science 2015;347:1002–6.
14. Jia G, Fu Y, Zhao X, Dai Q, Zheng G, Yang Y, et al. N6-methyladenosine in nuclear RNA is a major substrate of the obesity-associated FTO. Nat Chem Biol 2011;7:885–7.
15. Meyer KD, Saletore Y, Zumbo P, Elemento O, Mason CE, Jaffrey SR. Comprehensive analysis of mRNA methylation reveals enrichment in 3' UTRs and near stop codons. Cell 2012;149:1635–46.
16. World Health Organization. WHO laboratory manual for the examination and processing of human semen. 5th ed. Geneva: World Health Organization; 2010.

17. Menkveld R, Stander FS, Kotze TJ, Kruger TF, van Zyl JA. The evaluation of morphological characteristics of human spermatozoa according to stricter criteria. Hum Reprod 1990;5:586–92.
18. Evenson D, Jost L. Sperm chromatin structure assay for fertility assessment. Curr Protoc Cytom 2001;Chapter 7:Unit 7 13.
19. Van der Steeg JW, Steures P, Eijkemans MJ, F Habbema JD, Hompes PG, Kremer JA, et al. Role of semen analysis in subfertile couples. Fertil Steril 2011;95:1013–9.
20. Wang K, Li M, Hakonarson H. ANNOVAR: functional annotation of genetic variants from high-throughput sequencing data. Nucleic Acids Res 2010;38:e164.
21. Finn RD, Bateman A, Clements J, Coggill P, Eberhardt RY, Eddy SR, et al. Pfam: the protein families database. Nucleic Acids Res 2014;42:D222–30.
22. UniProt C. Activities at the Universal Protein Resource (UniProt). Nucleic Acids Res 2014;42:D191–8.
23. Liu X, Jian X, Boerwinkle E. dbNSFP v2.0: a database of human non-synonymous SNVs and their functional predictions and annotations. Hum Mutat 2013;34:E2393–402.
24. Sherry ST, Ward MH, Kholodov M, Baker J, Phan L, Smigielski EM, et al. dbSNP: the NCBI database of genetic variation. Nucleic Acids Res 2001;29:308–11.
25. ExAC. Exome Aggregation Consortium (ExAC) URL. Cambridge, MA, March, 2015. Available at: http://exac.broadinstitute.org/. Last accessed January 28, 2016.
26. Han Z, Niu T, Chang J, Lei X, Zhao M, Wang Q, et al. Crystal structure of the FTO protein reveals basis for its substrate specificity. Nature 2010;464:1205–9.
27. Forti G, Krausz C. Clinical review 100: Evaluation and treatment of the infertile couple. J Clin Endocrinol Metab 1998;83:4177–88.
28. Matzuk MM, Lamb DJ. The biology of infertility: research advances and clinical challenges. Nat Med 2008;14:1197–213.
29. Kosova G, Scott NM, Niederberger C, Prins GS, Ober C. Genome-wide association study identifies candidate genes for male fertility traits in humans. Am J Hum Genet 2012;90:950–61.
30. Steger K. Haploid spermatids exhibit translationally repressed mRNAs. Anat Embryol 2001;203:323–34.
31. Dominissini D, Moshitch-Moshkovitz S, Schwartz S, Salmon-Divon M, Ungar L, Osenberg S, et al. Topology of the human and mouse m6A RNA methylomes revealed by m6A-seq. Nature 2012;485:201–6.
32. Zhong S, Li H, Bodi Z, Button J, Vespa L, Herzog M, et al. MTA is an Arabidopsis messenger RNA adenosine methylase and interacts with a homolog of a sex-specific splicing factor. Plant Cell 2008;20:1278–88.
33. Kurowski MA, Bhagwat AS, Papaj G, Bujnicki JM. Phylogenomic identification of five new human homologs of the DNA repair enzyme AlkB. BMC Genomics 2003;4:48.
34. Klungland A, Dahl JA. Dynamic RNA modifications in disease. Curr Opin Genet Dev 2014;26C:47–52.
35. Hongay CF, Orr-Weaver TL. Drosophila Inducer of MEiosis 4 (IME4) is required for Notch signaling during oogenesis. Proc Natl Acad Sci U S A 2011;108:14855–60.
36. Berulava T, Ziehe M, Klein-Hitpass L, Mladenov E, Thomale J, Ruther U, et al. FTO levels affect RNA modification and the transcriptome. Eur J Hum Genet 2013;21:317–23.
37. Frayling TM, Timpson NJ, Weedon MN, Zeggini E, Freathy RM, Lindgren CM, et al. A common variant in the FTO gene is associated with body mass index and predisposes to childhood and adult obesity. Science 2007;316:889–94.
38. Gerken T, Girard CA, Tung YC, Webby CJ, Saudek V, Hewitson KS, et al. The obesity-associated FTO gene encodes a 2-oxoglutarate-dependent nucleic acid demethylase. Science 2007;318:1469–72.
39. Fischer J, Koch L, Emmerling C, Vierkotten J, Peters T, Bruning JC, et al. Inactivation of the Fto gene protects from obesity. Nature 2009;458:894–8.
40. Gulati P, Avezov E, Ma M, Antrobus R, Lehner P, O'Rahilly S, et al. Fat mass and obesity-related (FTO) shuttles between the nucleus and cytoplasm. Biosci Rep 2014;34.
41. Uhlen M, Fagerberg L, Hallstrom BM, Lindskog C, Oksvold P, Mardinoglu A, et al. Proteomics. Tissue-based map of the human proteome. Science 2015;347:12604–19.
42. Li W, Wu J, Kim SY, Zhao M, Hearn SA, Zhang MQ, et al. Chd5 orchestrates chromatin remodelling during sperm development. Nat Commun 2014;5:3812.
43. Labrecque R, Lodde V, Dieci C, Tessaro I, Luciano AM, Sirard MA. Chromatin remodelling and histone m RNA accumulation in bovine germinal vesicle oocytes. Mol Reprod Dev 2015;82:450–62.
44. Kotaja N, Sassone-Corsi P. The chromatoid body: a germ-cell-specific RNA-processing centre. Nat Rev Mol Cell Biol 2007;8:85–90.
45. Kotaja N, Bhattacharyya SN, Jaskiewicz L, Kimmins S, Parvinen M, Filipowicz W, et al. The chromatoid body of male germ cells: similarity with processing bodies and presence of Dicer and microRNA pathway components. Proc Natl Acad Sci U S A 2006;103:2647–52.
46. Wang X, Lu Z, Gomez A, Hon GC, Yue Y, Han D, et al. N6-methyladenosine-dependent regulation of messenger RNA stability. Nature 2014;505:117–20.
47. Kubo-Irie M, Matsumiya K, Iwamoto T, Kaneko S, Ishijima S. Morphological abnormalities in the spermatozoa of fertile and infertile men. Mol Reprod Dev 2005;70:70–81.
48. Barrett LW, Fletcher S, Wilton SD. Regulation of eukaryotic gene expression by the untranslated gene regions and other non-coding elements. Cell Mol Life Sci 2012;69:3613–34.
49. Hendrickson DG, Hogan DJ, McCullough HL, Myers JW, Herschlag D, Ferrell JE, et al. Concordant regulation of translation and mRNA abundance for hundreds of targets of a human microRNA. PLoS Biol 2009;7:e1000238.
50. Sood P, Krek A, Zavolan M, Macino G, Rajewsky N. Cell-type-specific signatures of microRNAs on target mRNA expression. Proc Natl Acad Sci U S A 2006;103:2746–51.
51. Pesole G, Mignone F, Gissi C, Grillo G, Licciulli F, Liuni S. Structural and functional features of eukaryotic mRNA untranslated regions. Gene 2001;276:73–81.
52. Feng C, Liu Y, Wang G, Deng Z, Zhang Q, Wu W, et al. Crystal structures of the human RNA demethylase Alkbh5 reveal basis for substrate recognition. J Biol Chem 2014;289:11571–83.
53. Meyre D, Proulx K, Kawagoe-Takaki H, Vatin V, Gutierrez-Aguilar R, Lyon D, et al. Prevalence of loss-of-function FTO mutations in lean and obese individuals. Diabetes 2010;59:311–8.
54. Boissel S, Reish O, Proulx K, Kawagoe-Takaki H, Sedgwick B, Yeo GS, et al. Loss-of-function mutation in the dioxygenase-encoding FTO gene causes severe growth retardation and multiple malformations. Am J Hum Genet 2009;85:106–11.
55. Smemo S, Tena JJ, Kim KH, Gamazon ER, Sakabe NJ, Gomez-Marin C, et al. Obesity-associated variants within FTO form long-range functional connections with IRX3. Nature 2014;507:371–5.
56. Tuttelmann F, Rajpert-De Meyts E, Nieschlag E, Simoni M. Gene polymorphisms and male infertility—a meta-analysis and literature review. Reprod Biomed Online 2007;15:643–58.

SUPPLEMENTAL FIGURE 1

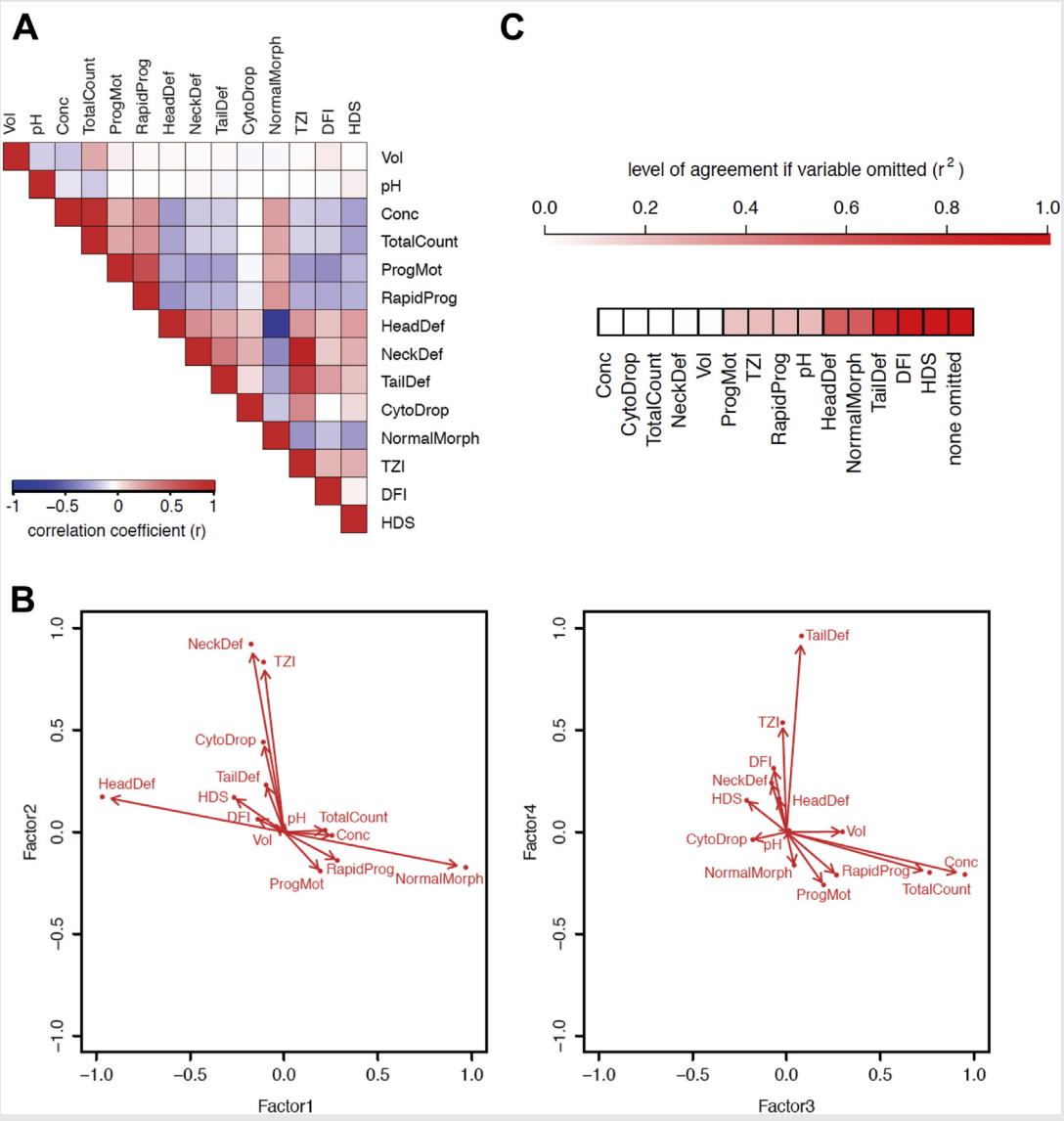

Reduction of highly correlated semen parameters with factor analysis. (**A**) Correlation matrix reveals multiple close correlations among semen parameters in men who are not azoospermic undergoing infertility work-up (n = 6,049). Color scale, Pearson's correlation coefficient. Conc = sperm concentration (million/mL); CytoDrop = presence of cytoplasmic droplets (%); DFI = DNA fragmentation index; HDS = high DNA stainability; HeadDef = irregular head morphology (%); NeckDef = irregular neck morphology (%); NormalMorph = sperm with normal morphology; ProgMot = progressive motile sperm (%); RapidProg = rapid progressively motile sperm (%); TailDef = irregular tail morphology (%); TotalCount = total sperm count (million); TZI = teratozoospermia index; Vol = volume (mL). (**B**) From 14 measured semen parameters, factor analysis extracts 4 unobserved, independent variables, also called factors, as linear combination of semen parameters. Here, linear coefficients, also called factor loadings, are plotted for each semen parameter. (**C**) Mean factor scores derived after omitting sperm parameters one-by-one were compared with the full model using the r^2 statistics. Omission of sperm parameters with large impact on factor analysis (e.g., concentration) yields models with low agreement with the models based on all parameters. Sensitivity analysis indicates that the factor was dominated by sperm concentration values, whereas the independent influence of chromatin parameters (DFI, HDS) was low.

Landfors. Sequencing of FTO *and* ALKBH5 *variants. Fertil Steril 2016.*

SUPPLEMENTAL FIGURE 2

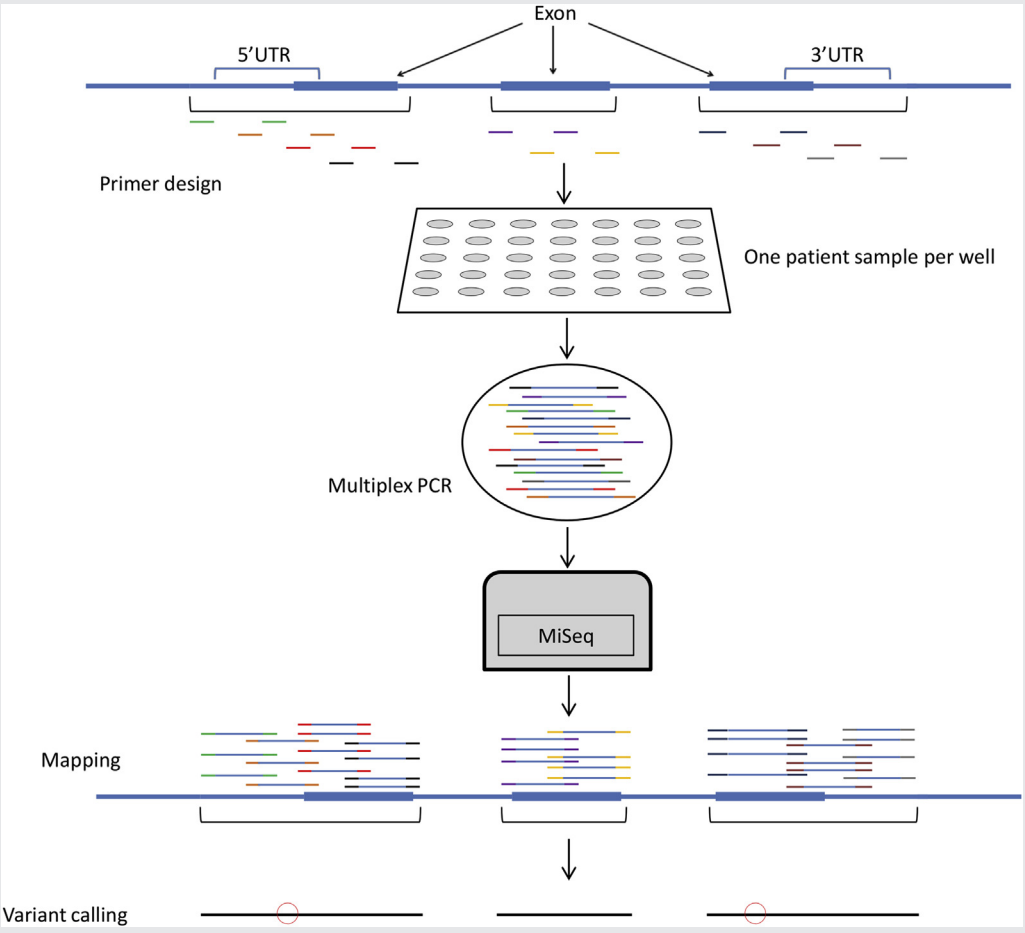

Schematic overview of sequencing design. Amplicons were designed to cover the exonic regions, splice sites and parts of the untranslated (UTR) regions. Sequencing was carried out using the Illumina MiSeq platform and variants were called with GATK's UnifiedGenotyper. *Red circles* illustrate identified variants. PCR = polymerase chain reaction.

Landfors. Sequencing of FTO *and* ALKBH5 *variants. Fertil Steril 2016.*

SUPPLEMENTAL FIGURE 3

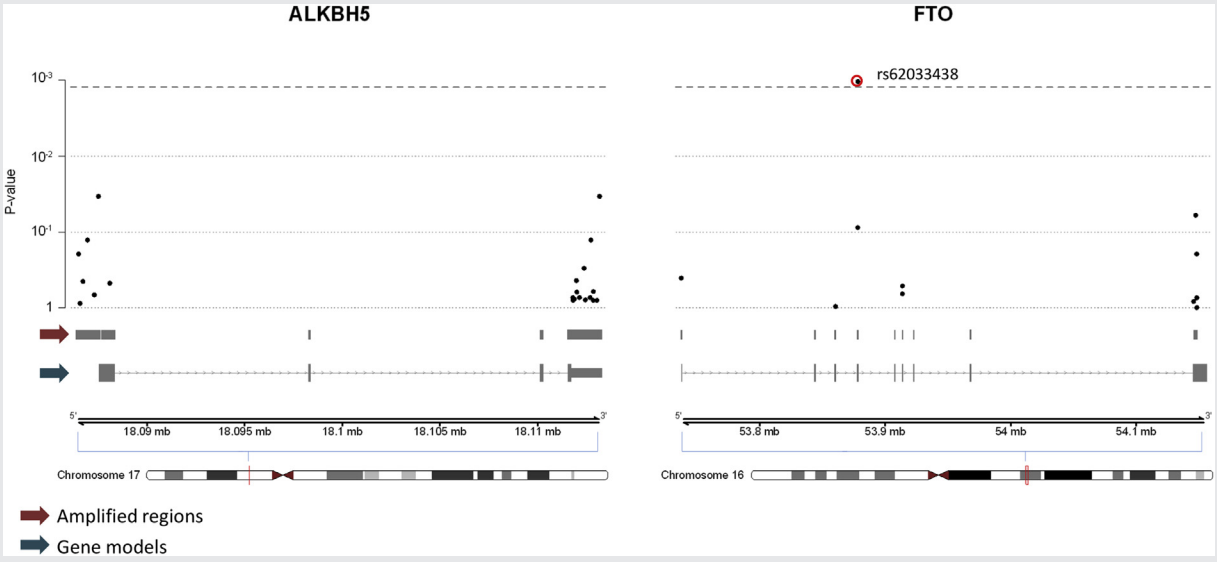

Amplified regions of *FTO* and *ALKBH5* with variant positions. In 77 men undergoing infertility work-up, we sequenced selected regions of ALKBH5 and FTO, located on chromosomes 17 and 16, respectively (*bottom*). Appropriate primers were designed to cover the 5′ and 3′ untranslated regions, exons, and neighboring intronic regions of ALKBH5 and FTO (gene models, *blue arrow*), and the amplified regions (*red arrow*) were sequenced on the Illumina MiSeq platform. The presence of sequence variants (*dots*) was related to semen quality using linear regression. Variant rs62033438 (*red circle*), located within the fourth intron of the FTO gene, achieved statistically significant association with semen quality (P=.00103; *dashed line* indicates Bonferroni-corrected α<0.05).

Landfors. Sequencing of FTO *and* ALKBH5 *variants. Fertil Steril 2016.*

SUPPLEMENTAL FIGURE 4

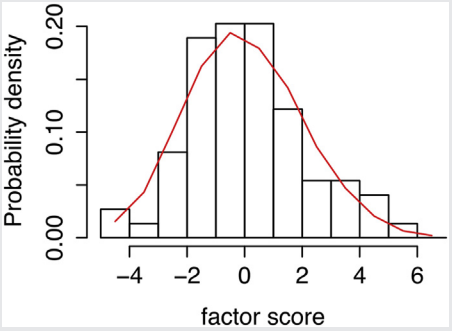

The group of men (n = 77) examined for genomic variants of ALKBH5 and FTO is representative of the population of men who are not azoospermic (n = 6,049). Factor analysis was used to extract 4 unobserved independent factors from 14 measured semen parameters in 6,049 men undergoing infertility work-up. The *red line* indicates population distribution of factor scores. The factor analysis model established in the larger population was subsequently applied to the sample of 77 men, and it resulted in indistinguishable sample distribution of factor scores (bar chart; Kolmogorov-Smirnov test, *P*=.79).

Landfors. Sequencing of FTO *and* ALKBH5 *variants. Fertil Steril 2016.*

SUPPLEMENTAL FIGURE 5

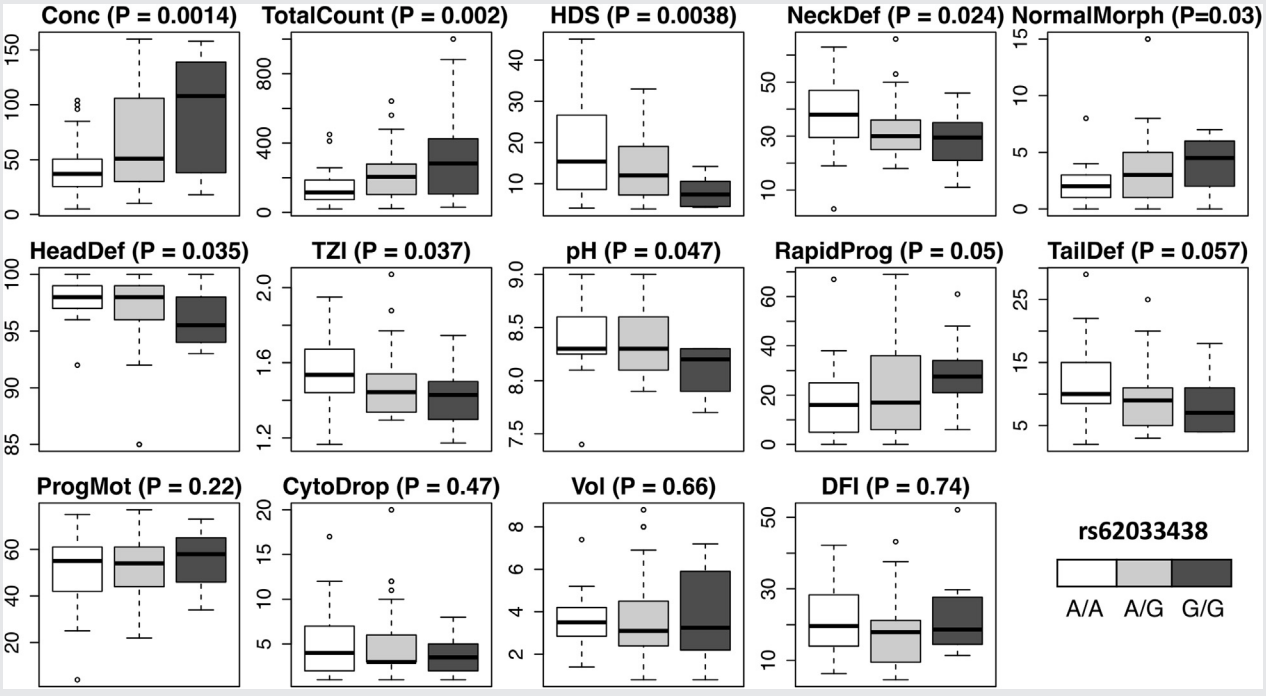

Association between semen parameters and the presence of FTO variant rs62033438. Semen parameters of men who are not azoospermic (n = 77) are grouped according to the strength of association with the presence of rs62033438 variant. Uncorrected *P* value, linear regression analysis. Conc = sperm concentration (million/mL); CytoDrop = presence of cytoplasmic droplets (%); DFI = DNA fragmentation index; HDS = high DNA stainability; HeadDef = irregular head morphology (%); NeckDef = irregular neck morphology (%); NormalMorph = sperm with normal morphology; ProgMot = progressive motile sperm (%); RapidProg = rapid progressively motile sperm (%); TailDef = irregular tail morphology (%); TotalCount = total sperm count (million); TZI = teratozoospermia index; Vol = volume (mL). *Boxes bottom right*: the observed variant A/A (*white*); heterozyogte A/G (*light gray*); wild-type G/G (*dark gray*). Box plot explanation: *upper horizontal line* of box, 75th percentile; *lower horizontal line* of box, 25th percentile; *horizontal bar* within box, median; *upper horizontal bar* outside box, 90th percentile; *lower horizontal bar* outside box, 10th percentile. *Circles* represent outliers.

Landfors. Sequencing of FTO *and* ALKBH5 *variants. Fertil Steril 2016.*